[9] Screening for Activators of the Wingless Type/Frizzled Pathway by Automated Fluorescent Microscopy

By KRISTEN M. BORCHERT, RACHELLE J. SELLS GALVIN, LAURA V. HALE, O. JOSEPH TRASK, DEBRA R. NICKISCHER, and KEITH A. HOUCK

Abstract

Development of means to screen primary human cells rather than established cell lines is important in improving the predictive value of cellular assays in drug discovery. We describe a method of using automated fluorescent microscopy to detect activators of the wingless type/Frizzled (Wnt/Fzd) pathway in primary human preosteoblasts. This technique relies on detection of endogenous β-catenin translocation to the nucleus as an indicator of pathway activation, requires only a limited number of primary cells, and is robust enough for automation and high-content, high-throughput screening. Identification of activators of the Wnt/Fzd pathway in human preosteoblasts may be useful in providing lead compounds for the treatment of osteoporosis.

Introduction

Developing effective means of screening primary human cells for phenotypic changes is an important goal in improving drug discovery research. Primary cells are more representative of *in vivo* physiology than established cell lines. During the process of cell line establishment, genetic and epigenetic changes occur that may influence the target being pursued in unknown ways (Baguley and Marshall, 2004; Horrocks *et al.*, 2003). Such changes may result in the generation of false-positive leads that are ineffective *in vivo,* as well as false negatives, eliminating potentially efficacious leads. Primary cells, particularly if cultured in the appropriate microenvironment, reduce the likelihood of such problems (Bissell *et al.*, 2002). However, as evidenced by the relative paucity of descriptions of use of primary human cells in screening campaigns, numerous obstacles exist to their successful implementation in screening assays. Some of these obstacles are beginning to be addressed. Although availability of primary cells previously required access to human tissue sources, a wide variety of cell types are now available from numerous sources. These cells can typically

METHODS IN ENZYMOLOGY, VOL. 414

0076-6879/06 $35.00
DOI: 10.1016/S0076-6879(06)14009-4

be passaged only a limited number of times, however. Together with their cost, this puts practical limits on how they can be used in drug discovery. In addition, engineering of these cells is challenging in that introducing reporter genes with plasmid DNA is often difficult and immortal cell lines cannot be created without likely losing the primary cell phenotype. Use of lentiviral vectors is one possibility for dealing with this problem (Verhoeyen and Cosset, 2004). Alternatively, a means of addressing both the limited cell availability and difficulty introducing reporter gene systems is by using a high-content screening approach relying on measurement of phenotypic changes by automated fluorescence microscopy. This chapter illustrates this approach using a system to measure activation of the wingless type/Frizzled (Wnt/Fzd) pathway in primary human preosteoblast cells as a screen for compounds with potential bone anabolic activity.

Our interest in the Wnt/Fzd pathway in a preosteoblast cell arose from the clear involvement of the pathway in regulation of bone phenotype. The Wnt family of secreted lipoproteins consists of 19 family members that regulate cell–cell signaling controlling proper patterning during embryogenesis (Logan and Nusse, 2004). Maintenance of tissue phenotype in the adult is another function and dysregulation results in pathologies, including cancer (Sparks *et al.*, 1998). Wnt binds to the seven-transmembrane domain receptor Fzd, a non-G-protein-coupled receptor family containing 10 members in human (Bhanot, 1996; Yang-Snyder, 1996). A coreceptor protein, low-density lipoprotein receptor-related protein (LRP) is required for signal transduction (Pinson 2000; Tamai *et al.*, 2000). Wnt binding to Fzd/LRP results in the transmission of signal through disheveled (DSH) to a protein complex that includes axin, glycogen synthase kinase-3β (GSK3β), adenomatous polyposis coli (APC), and the transcription factor β-catenin (Nelson, 2004; Wnt home page) and results in inhibition of the phosphorylation of β-catenin by GSK3β. This causes inhibition of ubiquitin-mediated degradation of β-catenin and stabilization of cytoplasmic levels of the protein. The increasing cytoplasmic level leads to subsequent nuclear translocation of β-catenin. There it binds to the transcription factor T-cell-specific transcription factor/lymphoid enhancer-binding factor-1 (TCF/LEF), yielding a new transcription factor complex capable of regulating a wide variety of genes involved in growth and differentiation (Cadigan, 1997; Giles, 2003).

Involvement of the Wnt/Fzd pathway in bone formation was shown through a number of genetic studies in both human and rodent. In humans, mutations in the coreceptor LRP5 yielded either marked cortical bone thickening for activating mutations (Boyden, 2002; Little, 2002) or osteoporosis pseudoglioma syndrome for inactivating ones (Gong, 2001). Deletion of LRP5 in mice decreased osteoblast formation and function, resulting in osteopenia (Kato, 2002). Transgenic mice expressing the activating mutation

had increased bone mass (Babij, 2003). A soluble, secreted decoy Wnt receptor, Fzd-related protein-1, caused increased trabecular bone formation when deleted in mice (Bodine, 2004). A pharmacological study of activation of the Wnt/Fzd pathway using inhibitors of GSK3β induced *de novo* bone formation and pronounced hypertrophy of osteoblasts (Kulkarni *et al.*, 2004).

Use of Primary Human Preosteoblasts

Although the Wnt/Fzd pathway could be manipulated pharmacologically through inhibition of GSK3β, this is a common node of a number of signal transduction pathways (Cohen and Goedert, 2004; Jope and Johnson, 2004). Thus, this may be too nonselective as a mechanism to safely induce increased bone formation as a treatment for osteoporosis. Because other known components of the Wnt/Fzd pathway are not typical druggable-type targets, we chose to pursue identification of activators of the pathway through a phenotypic screening approach without a specific molecular target selected a priori. With this approach, we thought it essential to choose a cell type representing the *in vivo* physiological state as accurately as possible so that relevant potential targets would be present. For these reasons, we developed an assay to measure activation of the Wnt/Fzd pathway through quantifying the nuclear translocation of β-catenin in primary human preosteoblast cells (Bi *et al.*, 2001). These cells were isolated as a subpopulation of stromal mesenchymal cells from the surface of femoral bone marrow and shown capable of being induced to differentiate into osteoblasts. Activation of the Wnt/Fzd pathway was quantified using the Cellomics (Pittsburgh, PA) Arrayscan IV automated fluorescent microscope system. The Cellomics ArrayScan system is described extensively in Williams *et al.* (2006).

Reagents and Materials

Human presosteoblast cells: Obtained by Dr. L.X. Bi, University of Texas Medical Branch, (Galveston, TX) from femoral long bone marrow in compliance with the National Institute of Health's requirements for human subjects (Bi, 2001)

Cell culture maintenance medium: MEM α (Gibco/Invitrogen, Carlsbad, CA) supplemented with 10% fetal calf serum (FCS) (Hyclone, Logan, UT) and 2 m*M* L-glutamine

Trypsin-versene (Biowhittaker, Walkersville, MD)

Dulbecco's phosphate-buffered saline (DPBS) (Biowhittaker)

Dimethyl sulfoxide (DMSO) (JT Baker, Phillipsburg, NJ)

96-well black viewplates (Perkin-Elmer, Wellesley, MA)

Indolemaleimide GSK3 inhibitor synthesized by Eli Lilly & Co. (Indianapolis, IN) (Engler *et al.*, 2004)
37% formaldehyde (Sigma-Aldrich, St. Louis, MO)
Hoescht 33352 (Sigma-Aldrich)
Triton X-100 and Tween-20 (Roche Biochemicals, Indianapolis, IN)
Mouse anti-β-catenin antibody (BD Biosciences, San Jose, CA)
Alexa-488 goat antimouse antibody (Molecular Probes/Invitrogen, Eugene, OR)
L cells and Wnt3A-expressing L cells [American Type Tissue Collection (ATCC) Manassas, VA]
G418 (Gibco/Invitrogen)
Centricon Plus 80 (polyethersulfone, molecular weight cutoff, 5000)

Preparation of L Cell Control- and Wnt3A-Conditioned Medium

1. Grow L cells to confluence in T-150 flasks.
2. Trypsinize and split 1:20 in 20 ml of medium without G418 in T-150 flasks.
3. Grow and condition medium for 4 days at 37° and 5% CO_2 in a humidified incubator.
4. Collect conditioned medium, sterile filter, and store at 4°. Refeed cells with 20 ml of medium.
5. Collect conditioned medium at 72 h, sterile filter, and combine with first collection.
6. Concentrate approximately five-fold with Centricon Plus 80 centrifugal filters, sterile filter, and store at 4°.

Primary Preosteoblast Cell Culture and Compound Screening

Due to the limited availability of these cells and the constraint to maximum passage number, cells should be expanded to provide a pool of cells sufficient for a screening campaign. These cells were found to be capable of being differentiated into osteoblasts until approximately passage 12 (data not shown). Therefore we expanded the cells and pooled, aliqouted, and cryopreserved a screening lot of cells at passage 5. Cells were found to respond best to Wnt3A-conditioned medium following at least 2 weeks of growth in culture after removal from cryopreservation. Therefore cells were maintained in T-150 flasks and passaged when nearly confluent for 2 to 4 weeks before being used in screening. Cells were not used past passage 11. Optimal cell density for measuring a response to Wnt3A-conditioned medium was determined to be approximately 2000 cells per well, which permitted

a good compromise between low enough density to permit imaging of individual, segmented cells and high enough density to minimize the number of fields required to be imaged to achieve a statistically relevant population (Borchert *et al.*, 2005).

1. Thaw aliquots of frozen cells and plate in T-150 flasks in MEM α/10% FCS/2 m*M* glutamine. Incubate at 37° and 5% CO_2 in a humidified incubator.
2. Trypsinize and passage at 1:10 when nearly confluent. Cells are ready for screening after 2 weeks in culture. Do not use past passage 11.
3. Dilute to 20,000 cells/ml in MEM α/0.5% FCS/2 m*M* glutamine.
4. Plate 2000 cells/well with a Multidrop (Thermo Electron, Boston, MA) or other liquid dispenser in a black, 96-well Packard viewplate.
5. Incubate overnight at 37° and 5% CO_2.
6. Dilute compounds in 96-well polystyrene plates with MEM α to 10× desired screening concentration immediately before treating cells. The DMSO concentration should not exceed 0.25% in the assay plate. Include appropriate positive (10 μM GSK3 inhibitor or 2.5-fold concentrated Wnt3A-conditioned medium) and negative (2.5% DMSO or 2.5-fold concentrated control L cell-conditioned medium) controls at 10× final concentration.
7. Using Multimek 96 (Beckman Coulter, Fullerton, CA) or other suitable liquid handler, dispense 11 μl of compound or conditioned medium per well.
8. Return plates to incubator for 4 h before processing for immunofluorescence.

Immunofluorescent Staining

In order to identify the subcellular localization of β-catenin, we used the immunofluorescent staining approach and the Arrayscan automated fluorescent microscope for detection. To simplify the assay protocol, we initially tested a primary antibody against human β-catenin directly conjugated with FITC. Although we were able to observe the nuclear translocation of β-catenin upon stimulation with Wnt3A-conditioned medium, there was a very low signal-to-background due to a significant level of background staining. Attempts to reduce background were unsuccessful so an indirect immunofluorescent staining using an Alexa 488 goat antimouse antibody was implemented. While more cumbersome due to the required two staining and washing steps, this significantly enhanced the signal-to-background ratio. The following steps were automated using a Multimek

for cell fixation and an MRD8 titrator (Titertek, Huntsville, AL) for immunofluorescent staining.

1. Following a 4-h incubation after compound treatment, aspirate medium from plates with Multimek and immediately add 100 μl 3.7% formaldehyde in DPBS, warmed to 37°, to fix cells; incubate 15 min at room temperature.
2. Using Multimek, wash cells twice with 100 μl DPBS.
3. Permeabilize cells with 100 μl 0.1% Triton X-100 in DPBS for 5 min.
4. Wash cells with 100 μl DPBS.
5. Add 50 μl of 1 μg/ml mouse anti-β-catenin in DPBS and incubate at room temperature for 1 h.
6. Wash cells with 100 μl blocking buffer (0.1% Tween-20 in DPBS).
7. Add 100 μl blocking buffer and incubate 15 min at room temperature.
8. Wash once with 100 μl DPBS.
9. Add 100 μl of DPBS containing 10 μg/ml Alexa 488 goat antimouse antibody and 2 μg/ml Hoescht 33342 and incubate 1 h at room temperature.
10. Wash once with blocking buffer and twice with DPBS.
11. Add 100 μl of DPBS and seal plates; read on ArrayScan immediately or store at 4° in the dark up to 4 weeks.

Imaging and Quantitation of Nuclear Translocation

Fixed and stained plates were imaged on the Cellomics ArrayScan IV using the nuclear translocation algorithm (Fig. 1). The algorithm identifies a cell by the nuclear Hoescht 33342 dye and draws a mask around the boundaries of the nucleus. A copy of this mask is then dilated as defined by the user to form the inner cytoplasm ring mask outside of the boundaries of the nucleus. Next a copy of this mask is expanded to form the outer cytoplasmic ring mask. Image analysis measurements, including size, shape, and fluorescent intensity of the target protein β-catenin as marked by Alexa488 in the nuclear and cytoplasm compartments, are made. The fluorescence difference between the nucleus and the cytoplasm is quantified and reported per individual cell or as average of the entire population in the field. Starting from the default protocol, the algorithm was modified to reduce artifacts induced by the fixing and staining technique and to accommodate the specific morphology of these cells. Specifically, the automated fixing and staining resulted in a significant number of cells that had folded over themselves, resulting in artificially high fluorescent readings. Also, some overlapping cells were seen with resulting high fluorescence.

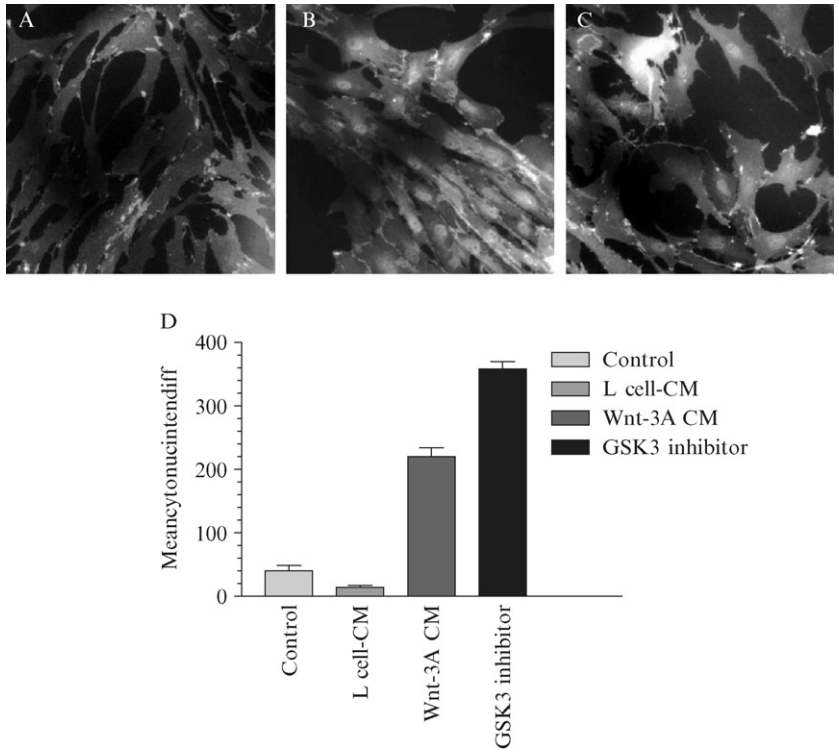

FIG. 1. Images of staining of β-catenin in human preosteoblasts treated with (A) control L cell-conditioned medium, (B) Wnt-3A-conditioned medium, or (C) GSK3 inhibitor. Quantitation of the degree of nuclear translocation of the β-catenin is shown in D.

We were unsuccessful in using morphologic parameters to exclude these cells from analysis but were able to do so setting upper limits on the total fluorescent intensity measurements in the target channel. Cells with folded nuclei were excluded by setting the upper limit of the parameter (nuclear fluorescence intensity/nuclear area) at that which would include approximately 99% of morphologically normal cells in a positive control population (treated with GSK3β inhibitor). Cells with overlapping cytoplasm were excluded by setting an upper limit on total fluorescence intensity in the target channel to a value that includes 99% of nonoverlapping cells in a negative control population. Finally, the cytoplasmic ring was set as a dilation of two pixels due to the relatively elongated shape of the cells and narrow band of cytoplasm that could be imaged outside the nucleus.

Translocation of β-catenin to the nucleus was reported as the difference in Alexa 488 fluorescence intensity between the nuclear area and the cytoplasmic area and was designated MeanNucCytoIntenDiff (Fig. 1D).

1. Set up ArrayScan IV with 10×/0.45NA Zeiss objective.
2. Set to default nuclear translocation algorithm and adjust parameters to measure 100 objects per well or up to a maximum of six fields per well.
3. Image positive and negative controls using the default nuclear translocation algorithm. Adjust algorithm as described earlier to exclude cells with undesirable morphologies.
4. Read plates.

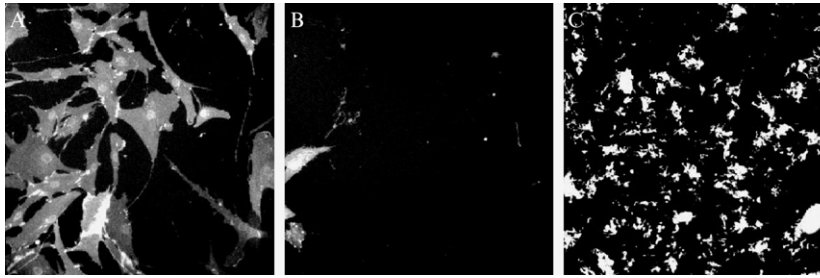

FIG. 2. Example of images of wells that were calculated as active by the cytoplasm to nuclear translocation algorithm illustrating (A) a true hit, (B) a false positive due to cytotoxicity, and (C) a false positive due to a fluorescent compound.

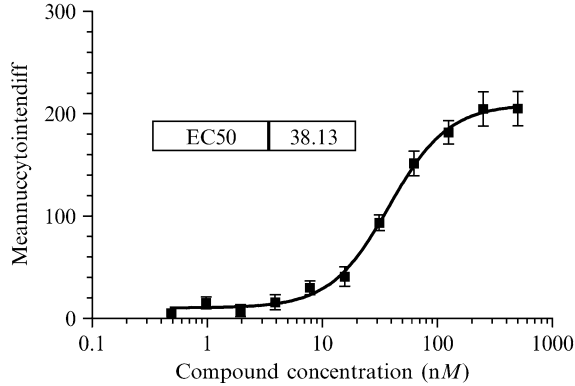

FIG. 3. Results of a confirmation assay done as a concentration–response curve for cytoplasm to nuclear translocation of β-catenin in primary human preosteoblasts.

Data Analysis

One of the advantages of high-content screening is the ability to look at a variety of result parameters that can be used to exclude false-positive results early in the screening process. For example, cytotoxicity often resulted in small, rounded-up cells with high fluorescence intensity or peculiar fluorescent accumulations in the target channel that the algorithm sometimes interpreted as an active well (Fig. 2). Generally, these wells had fewer than 100 objects counted per well and such wells are found easily by sorting data based on valid object count. Occasionally, compounds fluorescent in the target channel were noted that also resulted in false positives (Fig 2). These can be excluded by examining images from positive wells, in particular those with MeanNucCytoIntenDiff much greater than the positive control. Compounds with apparent real activity were confirmed in concentration–response format. As shown in Fig. 3, the resulting response curve gives reassurance as to normal pharmacological behavior of the compound and inspection of associated images can rule out artifacts. These hits were then advanced to additional testing, including counterscreening and mechanism of action studies.

Acknowledgments

We thank Dr. Liangxiang Bi for the human preosteoblast cells and Robin Gonyier, Ann McFarland, and Jonathan Gibbons for valuable technical assistance.

References

Babij, P., Zhao, W., Small, C., Kharode, Y., Yaworsky, P. J., Bouxsein, M. L., Reddy, P. S., Bodine, P. V., Robinson, J. A., Bhat, B., Marzolf, J., Moran, R. A., and Bex, F. (2003). High bone mass in mice expressing a mutant LRP5 gene. *J. Bone Miner. Res.* **18,** 960–974.

Baguley, B. C., and Marshall, E. S. (2004). *In vitro* modelling of human tumour behaviour in drug discovery programmes. *Eur. J. Cancer* **40,** 794–801.

Bhanot, P., Brink, M., Samos, C. H., Hsieh, J. C., Wang, Y., Macke, J. P., Andrew, D., Nathans, J., and Nusse, R. (1996). A new member of the frizzled family from Drosophila functions as a Wingless receptor. *Nature* **382,** 225–230.

Bi, L. X., Yngve, D., Buford, W. L., and Mainous, E. (2001). Isolation and characterization of preosteoblastic cells from human long bone marrow. *J. Bone Miner. Res.* **19**(Suppl. 1), SA050.

Bissell, M. J., Radisky, D. C., Rizki, A., Weaver, V. M., and Petersen, O. W. (2002). The organizing principle: Microenvironmental influences in the normal and malignant breast. *Differentiation* **70,** 537–546.

Bodine, P. V., Zhao, W., Kharode, Y. P., Bex, F. J., Lambert, A. J., Goad, M. B., Gaur, T., Stein, G. S., Lian, J. B., and Komm, B. S. (2004). The Wnt antagonist secreted frizzled-related protein-1 is a negative regulator of trabecular bone formation in adult mice. *Mol. Endocrinol.* **18,** 1222–1237.

Borchert, K. M., Galvin, R. J. S., Frolik, C. A., Hale, L. V., Gonyier, R., Trask, O. J., Nickischer, D. R., and Houck, K. A. (2005). Phenotypic screening for activators of the wnt/frizzled pathway in primary human osteoblasts. *Assay Drug Dev. Technol.* **3,** 133–141.

Boyden, L. M., Mao, J., Belsky, J., Mitzner, L., Farhi, A., Mitnick, M. A., Wu, D., Insogna, K., and Lifton, R. P. (2002). High bone density due to a mutation in LDL-receptor-related protein 5. *N. Engl. J. Med.* **346,** 1513–1521.

Cadigan, K. M., and Nusse, R. (1997). Wnt signaling: A common theme in animal development. *Genes Dev.* **11,** 3286–3305.

Cohen, P., and Goedert, M. (2004). GSK3 inhibitors: Development and therapeutic potential. *Nature Rev. Drug Discov.* **3,** 479–487.

Engler, T. A., Henry, J. R., Malhotra, S., Cunningham, B., Furness, K., Brozinick, J., Burkholder, T. P., Clay, M. P., Clayton, J., Diefenbacher, C., Hawkins, E., Iversen, P. W., Li, Y., Lindstrom, T. D., Marquart, A. L., McLean, J., Mendel, D., Misener, E., Briere, D., O'Toole, J. C., Porter, W. J., Queener, S., Reel, J. K., Owens, R. A., Brier, R. A., Eessalu, T. E., Wagner, J. R., Campbell, R. M., and Vaughn, R. (2004). Substituted 3-imidazo[1,2-a]pyridin-3-yl-4-(1,2,3,4-tetrahydro-[1,4]diazepino-[6,7,1-hi]indol-7-yl)pyrrole-2,5-diones as highly selective and potent inhibitors of glycogen synthase kinase-3. *J. Med. Chem.* **47,** 3934–3937.

Giles, R. H., van Es, J. H., and Clevers, H. (2003). Caught up in a Wnt storm: Wnt signaling in cancer. *Biochim. Biophys. Acta* **1653,** 1–24.

Gong, Y., Slee, R. B., Fukai, N., Rawadi, G., Roman-Roman, S., Reginato, A. M., Wang, H., Cundy, T., Glorieux, F. H., Lev, D., Zacharin, M., Oexle, K., Marcelino, J., Suwairi, W., Heeger, S., Sabatakos, G., Apte, S., Adkins, W. N., Allgrove, J., Arslan-Kirchner, M., Batch, J. A., Beighton, P., Black, G. C., Boles, R. G., Boon, L. M., Borrone, C., Brunner, H. G., Carle, G. F., Dallapiccola, B., De Paepe, A., Floege, B., Halfhide, M. L., Hall, B., Hennekam, R. C., Hirose, T., Jans, A., Juppner, H., Kim, C. A., Keppler-Noreuil, K., Kohlschuetter, A., LaCombe, D., Lambert, M., Lemyre, E., Letteboer, T., Peltonen, L., Ramesar, R. S., Romanengo, M., Somer, H., Steichen-Gersdorf, E., Steinmann, B., Sullivan, B., Superti-Furga, A., Swoboda, W., van den Boogaard, M. J., Van Hul, W., Vikkula, M., Votruba, M., Zabel, B., Garcia, T., Baron, R., Olsen, B. R., and Warman, M. L. (2001). LDL receptor-related protein 5 (LRP5) affects bone accrual and eye development. *Cell* **107,** 513–523.

Horrocks, C., Halse, R., Suzuki, R., and Shepherd, P. R. (2003). Human cell systems for drug discovery. *Curr. Opin. Drug Discov. Devel.* **6,** 570–575.

Jope, R. S., and Johnson, G. V. (2004). The glamour and gloom of glycogen synthase kinase-3. *Trends Biochem. Sci.* **29,** 95–102.

Kato, M., Patel, M. S., Levasseur, R., Lobov, I., Chang, B. H., Glass, D. A., 2nd, Hartmann, C., Li, L., Hwang, T. H., Brayton, C. F., Lang, R. A., Karsenty, G., and Chan, L. (2002). Cbfa1-independent decrease in osteoblast proliferation, osteopenia, and persistent embryonic eye vascularization in mice deficient in Lrp5, a Wnt coreceptor. *J. Cell. Biol.* **157,** 303–314.

Kulkarni, N. H., Liu, M., Halladay, D. L., Frolik, C. A., Engler, T. A., Helvering, L. M., Wei, T., Kriauciunas, A., Martin, T. J., Sato, M., Bryant, H. U., Onyia, J. E., and Ma, Y. L. (2006). An orally bioavailable GSK3 alpha-beta dual inhibitor increases markers of cellular differentiation *in vitro* and bone mass *in vivo*. *J. Bone Miner. Res.* **21,** 910–920.

Little, R. D., Carulli, J. P., Del Mastro, R. G., Dupuis, J., Osborne, M., Folz, C., Manning, S. P., Swain, P. M., Zhao, S. C., Eustace, B., Lappe, M. M., Spitzer, L., Zweier, S., Braunschweiger, K., Benchekroun, Y., Hu, X., Adair, R., Chee, L., FitzGerald, M. G., Tulig, C., Caruso, A., Tzellas, N., Bawa, A., Franklin, B.,

McGuire, S., Nogues, X., Gong, G., Allen, K. M., Anisowicz, A., Morales, A. J., Lomedico, P. T., Recker, S. M., Van Eerdewegh, P., Recker, R. R., and Johnson, M. L. (2002). A mutation in the LDL receptor-related protein 5 gene results in the autosomal dominant high-bone-mass trait. *Am. J. Hum. Genet.* **70,** 11–19.

Logan, C. Y., and Nusse, R. (2004). The Wnt signaling pathway in development and disease. *Annu. Rev. Cell Dev. Biol.* **20,** 781–810.

Pinson, K. I., Brennan, J., Monkley, S., Avery, B. J., and Skarnes, W. C. (2000). An LDL-receptor-related protein mediates Wnt signaling in mice. *Nature* **407,** 535–538.

Sparks, A. B., Morin, P. J., Vogelstein, B., and Kinzler, K. W. (1998). Mutational analysis of the APC/beta-catenin/Tcf pathway in colorectal cancer. *Cancer Res.* **58,** 1130–1134.

Tamai, K., Semenov, M., Kato, Y., Spokony, R., Liu, C., Katsuyama, Y., Hess, F., Saint-Jeannet, J. P., and He, X. (2000). LDL-receptor-related proteins in Wnt signal transduction. *Nature* **407,** 530–535.

Verhoeyen, E., and Cosset, F. L. (2004). Surface-engineering of lentiviral vectors. *J. Gene Med.* **6**(Suppl. 1), S83–S94.

Williams, R. G., Kandasamy, R., Nickischer, D., Trask, O. J., Laethem, C., Johnston, P. A., and Johnston, P. A. (2006). Generation and characterization of a stable MK2-EGFP cell line and subsequent development of a high-content imaging assay on the Cellomics ArrayScan platform to screen for p38 mitogen-activated protein kinase inhibitors. *Methods Enzymol.* **414**(this volume).

[10] A Live Cell, Image-Based Approach to Understanding the Enzymology and Pharmacology of 2-Bromopalmitate and Palmitoylation

By IVANA MIKIC, SONIA PLANEY, JUN ZHANG, CAROLINA CEBALLOS, TERRI SERON, BENEDIKT VON MASSENBACH, RACHAEL WATSON, SCOTT CALLAWAY, PATRICK M. MCDONOUGH, JEFFREY H. PRICE, EDWARD HUNTER, and DAVID ZACHARIAS

Abstract

The addition of a lipid moiety to a protein increases its hydrophobicity and subsequently its attraction to lipophilic environments like membranes. Indeed most lipid-modified proteins are localized to membranes where they associate with multiprotein signaling complexes. Acylation and prenylation are the two common categories of lipidation. The enzymology and pharmacology of prenylation are well understood but relatively very little is known about palmitoylation, the most common form of acylation. One distinguishing characteristic of palmitoylation is that it is a dynamic modification. To understand more about how palmitoylation is regulated,

METHODS IN ENZYMOLOGY, VOL. 414 0076-6879/06 $35.00

DOI: 10.1016/S0076-6879(06)14010-0